

# Through-focus Scanning Optical Microscopy

Ravikiran Attota\*, Ronald G. Dixson, and András E. Vladár

National Institute of Standards and Technology, Gaithersburg, MD 20899, USA

## ABSTRACT

Through-focus scanning optical microscopy (TSOM) is another ‘scanning’ based method that provides **three-dimensional** information (i.e. the size, shape and location) about micro- and nanometer-scale structures. TSOM, based on a conventional optical microscope, achieves this by acquiring and analyzing a set of optical images collected at various focus positions going through focus (from above-focus to under-focus). The measurement sensitivity is comparable to what is possible with typical light scatterometry, SEM and AFM. One of the unique characteristics of the TSOM method is its ability to separate different dimensional differences (i.e. ability to distinguish, for example, linewidth difference from line height difference), and hence is expected to reduce measurement uncertainty. TSOM holds the promise of high-throughput, through comparative measurement applications for wide variety of application areas with potentially significant savings and yield improvements.

**Keywords:** TSOM, through focus, optical microscope, nanometrology, process control, nanomanufacturing, nanoparticles, overlay metrology, critical dimension, defect analysis, dimensional analysis, MEMS, NEMS, photonics

## 1 INTRODUCTION

The demand on tools to make 3D measurements at the nanoscale is very high as dimensional information at the nanoscale is required to enable progress in nanotechnology and nanoscience [1,2]. ‘Scanning’ based tools are being increasingly used for nanoscale applications. Several tools, such as the atomic force microscope (AFM), scanning tunneling microscope (STM), and scanning electron microscope (SEM) are routinely used to provide measurements at this scale. Optics based scanning tools, such as near-field scanning optical microscope (NSOM), are also available for nanoscale applications.

It is often assumed that optical microscopes are not well suited for dimensional measurements of features that are smaller than half the wavelength of illumination (200 nm sized features in the visible region) due to diffraction [3]. However, this limitation can be circumvented by (i) considering the image as a dataset (or signal) that represents the target, (ii) using a set of through-focus images instead of one “best focus” image, and (iii) making use of highly developed optical models [4-6]. Based on this and on the observation of a distinct signature for different parametric variations, we introduced a new optical method for nanoscale dimensional analysis with nanometer sensitivity for three-dimensional, nano-sized targets using a conventional brightfield optical microscope [7-15]: through-focus scanning optical microscopy (TSOM). TSOM is applicable to three-dimensional targets (where a single “best focus” may be impossible to define), thus enabling it to be used for a wide range of target geometries and application areas.

Through-focus optical information was used before for several applications. Most frequently it has been in use to find the best-focus image position by evaluating contrast in the image. Confocal microscopy is another method that makes use of through-focus optical image information. In this method, out-of-focus optical image information present in the

---

\* Corresponding author: [ravikiran.attota@nist.gov](mailto:ravikiran.attota@nist.gov); phone: 1 301 975 5750

through-focus images is selectively discarded to form a 3D confocal image. It was found that the through-focus contrast in the image of isolated line gratings was sensitive to the line width (CD) [16,17]. In these type of studies, the plot of contrast in the profile as a function of focus position was termed as “through-focus focus metric”. CD analysis was performed by studying variations in the through-focus focus metric profile. As a visual aid for CD analysis using through-focus focus metric, through-focus optical cross sectional intensity profiles were stacked to form an image similar to the 2D TSOM images used in the current study in Ref. [18]. Through-focus optical differential images were also used to study defects [19]. As will be seen in the following sections, TSOM method uses differential TSOM images (i.e differential cross sectional intensity images) as opposed to differential images as used in this defect analysis work.

In the TSOM method, through-focus images are stacked as a function of focus position resulting in a 3D space containing optical information. From this 3D image space, cross sectional 2D TSOM images are extracted through the location of interest in any given orientation. In the TSOM method the entire 3D optical information is acquired and preserved for dimensional analysis. Neither the out-of-focus optical information is discarded, as in Confocal microscopy, nor is the intensity profile reduced to a number, as in the through-focus focus metric method.

## 2 METHOD TO CONSTRUCT A TSOM IMAGE

The TSOM method requires a conventional brightfield optical microscope with a digital camera to capture images, and a motorized stage to move the target through the focus. Fig. 1 demonstrates the method to construct TSOM images using an isolated line as a target. Simulated optical images are used here to illustrate the method. Optical images are acquired as the target is scanned through the focus of the microscope (along the  $z$ -axis) as shown in Figs. 1(a) & 1(b). Each scan position results in a slightly different two-dimensional intensity image (Fig. 1(c)). The acquired optical images are stacked at their corresponding scan positions, creating a three-dimensional TSOM image, where the  $x$  and the  $y$ -axes represent the spatial position on the target and the  $z$ -axis the scanned focus position. In this 3D space, each location has a value corresponding to its optical intensity. The optical intensities in a plane (e.g., the  $xz$  plane) passing through the location of interest on the target (e.g., through the center of the line) can be conveniently plotted as a 2D image, resulting in a 2D-TSOM image as shown in Fig. 1(e), where the  $x$  axis represents the spatial position on the target (in  $x$ ), the  $y$  axis represents the focus position, and the color scale represents the optical intensity. Note that the intensity (color) axis is typically rescaled for each image. For 3D targets, appropriate 2D-TSOM images are selected for dimensional analysis. In this paper, we use “TSOM image” to refer to these 2D-TSOM cross-sectional images.

## 3 CHARACTERISTICS OF TSOM IMAGES

### 3.1 TSOM Images Change with Target

The TSOM images vary substantially for different types of targets. This variation is illustrated in Fig. 2 for four types of targets, using optical modeling simulations. An isolated line, measured using a reflection-based optical microscope, is shown in Fig. 2(a). A finite dense array with 9 lines produces the TSOM image in Fig. 2 (b). This target has a pitch of 105 nm, and the simulation was done using 193 nm. In-chip overlay targets must be small so that they can be placed in the active area. The TSOM image for an in-chip target at  $\lambda = 193$  nm is shown in Fig. 2(c). A TSOM image may also be produced for transmission microscopy; a photomask target in a transmission mode microscope at  $\lambda = 365$  nm is shown in Fig. 2(d). This target has a chrome line on a quartz substrate.

### 3.2 Differential TSOM Images Appear to be Distinct for Different Dimensional Changes

A small change in the dimension of a target produces a corresponding change in the TSOM image. Comparing two TSOM images from different targets, one can identify differences between the targets. In the current analysis we demonstrate the approach for an isolated line (i.e., a line several wavelengths away from nearby features). Although one can compare and identify changes in different ways, here we present a method based on a differential TSOM image. For example, an isolated 2D line produces distinct differential TSOM images for line width, line height, and sidewall angle differences as shown in Figs. 3(a), 3(b), and 3(c), respectively. In this example the differential TSOM images facilitate identification of the dimensions that are different between these nanoscale targets.

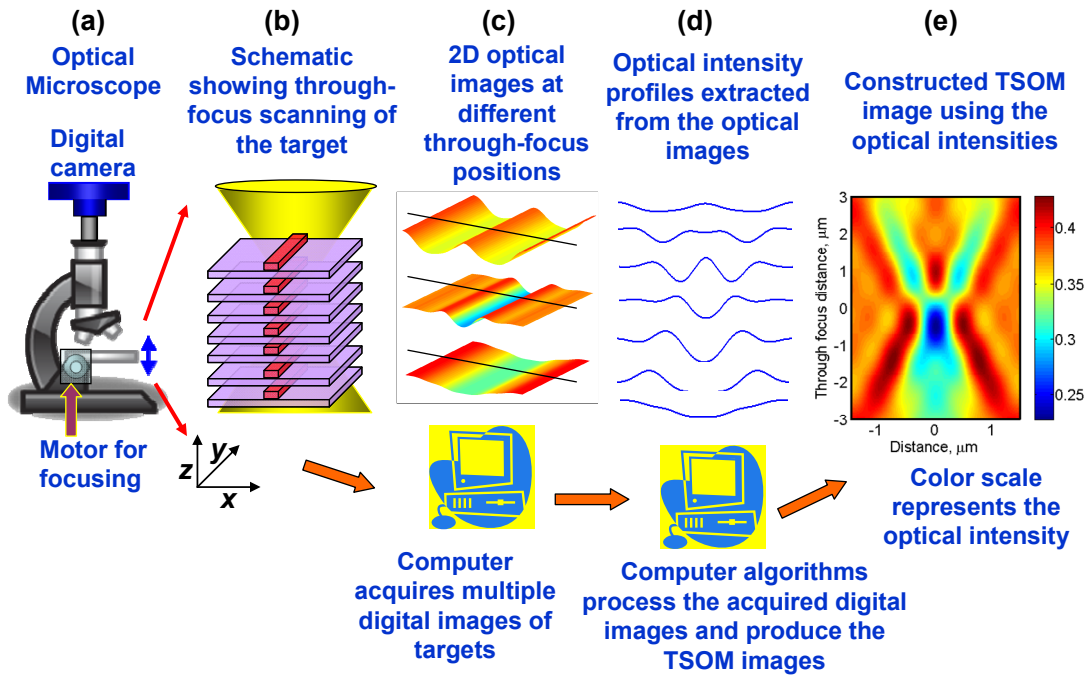


Figure 1. Method to construct TSOM images using a conventional optical microscope.

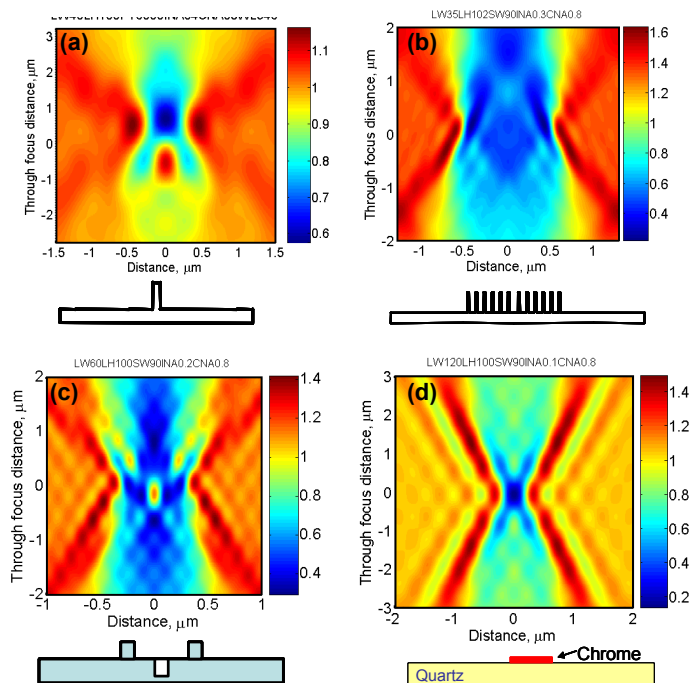


Figure 2. Simulated TSOM images for (a) an isolated Si line on a Si substrate (Line width = 40 nm, Line height = 100 nm, Illumination NA = 0.4, Collection NA = 0.8, and Illumination wavelength = 546 nm), (b) a finite dense Si array on a Si substrate (Number of lines = 9, Line width = 35 nm, Pitch = 105 nm, Line height = 100 nm, Illumination NA = 0.3, Collection NA = 0.8, and Illumination wavelength = 193 nm), (c) an in-chip Si line on a Si substrate overlay target (Linewidth = 60 nm, Line height = 100 nm, Trench width = 60 nm, Trench depth = 100 nm, Distance between the lines = 400 nm, Illumination NA = 0.2, Collection NA = 0.8, and Illumination wavelength = 193 nm), and (d) a chrome line on a quartz substrate photomask in transmission microscope mode (Linewidth = 120 nm, Line height = 100 nm, Illumination NA = 0.1, Collection NA = 0.8, Illumination wavelength = 365 nm).

The following observations can be made from the differential TSOM images. For the simulations shown, a small change in the dimension of the target can be identified using this method. However, sensitivity to small dimensional changes will depend on the measurement noise, sensitivity, and monotonic response. The simulation data show that a small change in the line height, the linewidth, or the sidewall angle show qualitatively distinct differential TSOM image responses. We have confirmed similar simulation-based results for several different types of targets.

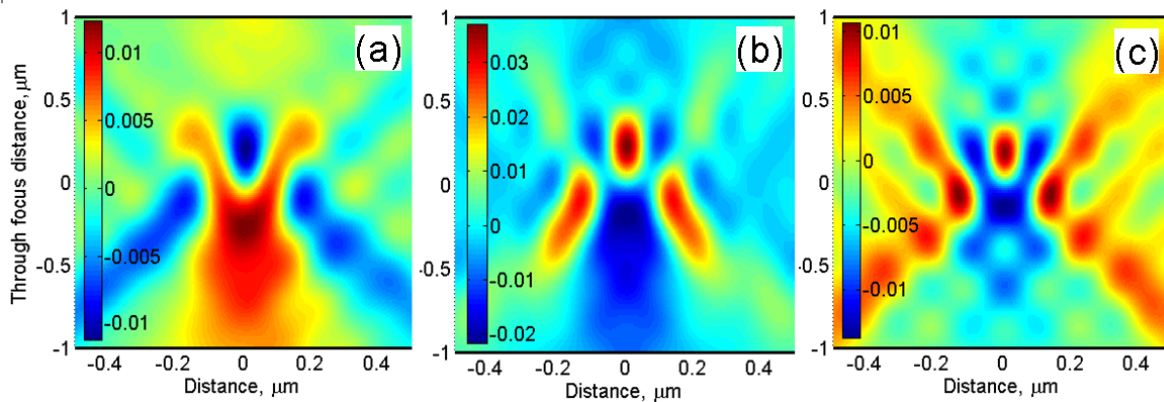


Figure 3. Simulated differential TSM images obtained for the 2D isolated line target shown in Fig. 1(b) for (a) 2.0 nm difference in the line width (42 nm and 40 nm), (b) 2.0 nm difference in the line height (82 nm and 80 nm), and (c) 2.0° difference in the sidewall angle (90° and 88°).

### 3.3 Differential TSM Images are Qualitatively Similar for Differences in the Same Dimension

As shown above, different dimensional changes (i.e., width or height) produce qualitatively distinct differential TSM images. However, for different magnitude changes of the same dimension, the differential TSM images appear qualitatively similar. Figs 4(a) and (b) present differential TSM images for 2.0 nm and 4.0 nm differences in linewidth, respectively, in an isolated line. These simulations yield qualitatively similar appearing differential TSM images. We performed the same analysis for several different types of targets under different conditions. In all the cases tested, we observed similar behavior, which holds true as long as the difference in the dimensional magnitude is smaller than the dimension of the target. It is also important to note that the qualitative differences in the differential TSM images for various dimensional changes (e.g., linewidth vs. line height) are much stronger than the differences in the differential TSM images for various magnitudes of change in the same dimensional parameter (1 nm vs. 2 nm linewidths).

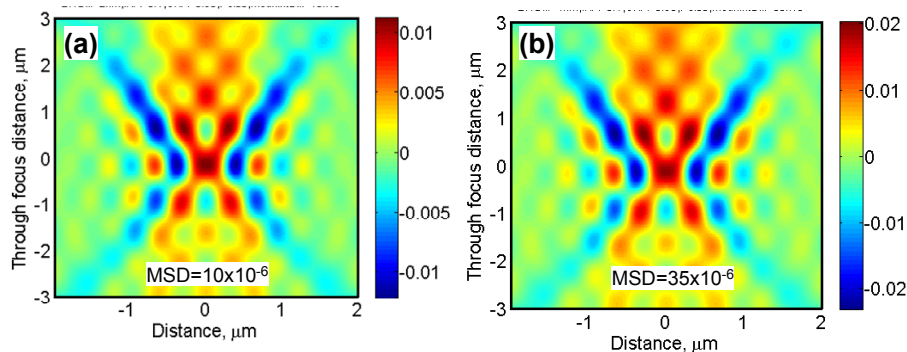


Figure 4. Simulated differential TSM image obtained for (a) the linewidths of 102 nm and 100 nm (2.0 nm difference), and (b) the linewidths of 104 nm and 100 nm (4.0 nm difference). Isolated line, Line height = 100 nm, Illumination NA = 0.25, Collection NA = 0.95, Illumination wavelength = 546 nm, Si line on Si substrate.

### 3.4 Integrated Optical Intensity of a Differential TSOM Image Indicates the Magnitude of the Dimensional Difference

Integrated optical intensity of a differential TSOM image can be evaluated in various ways. In the current work, we use two methods. Both can be used to quantify the magnitude of the difference for a single parameter. The first method is the “mean square difference” (*MSD*), which is defined here as,

$$MSD_{AB} = \frac{1}{N} \sum_{i=1}^N (A_i - B_i)^2$$

Where A and B are the TSOM images from two targets, and n is the total number of pixels in the image. Differences of 2.0 nm and 4.0 nm in the linewidths of an isolated line (Fig. 4) produce *MSD* values of  $10.0 \times 10^{-6}$  and  $35.0 \times 10^{-6}$ , respectively. In this example the *MSD* values increased in direct relationship to the magnitude of the dimensional differences. However, the amount of increase depends on the individual case. For consistent results and comparison, the total number of pixels in the images, the selected x-axis distance, and the focus range must be kept constant.

The second method is “mean difference” (*MD*), which is defined as follows:

$$MD_{AB} = \frac{1}{N} \sum_{i=1}^N |A_i - B_i|$$

Both *MSD* and *MD* are used appropriately where needed.

### 3.5 TSOM Images Appear to be Unique

We tested the uniqueness of TSOM images for a small parameter space using simulations. For this, we simulated a small library of TSOM images for linewidths varying from 145 nm to 155 nm and line heights varying from 125 nm to 135 nm. We used a 1.0 nm step increment for both the linewidth and the line height to produce a total of 121 simulation combinations. We then generated another set of “unknown” target simulations, the dimensions of which do not exactly match that of the targets in the library, as shown in the table in Fig. 5. These “unknown” targets were then compared to the library by evaluating the *MSD* values of their differential TSOM images. A plot of the *MSD* values thus obtained is shown in Fig. 5 for the linewidth of 146.2 nm and the line height of 233.8 nm. The minimum *MSD* value gives the best matched target. The best matched targets for the three unknown targets are also in Fig. 5. The uniqueness and agreement is good for these simulated images, but must yet be verified experimentally.

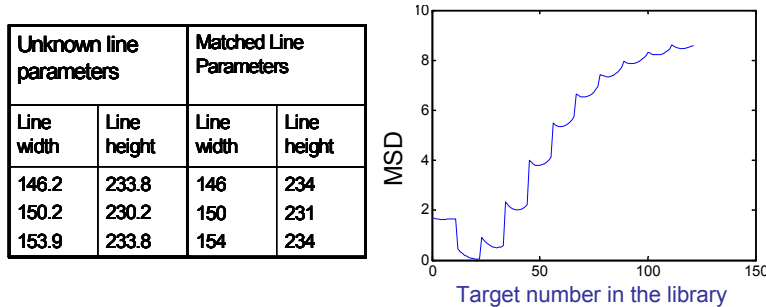


Figure 5. Demonstration of the uniqueness test using simulations. (a) Table showing the unknown line parameters and the matched line parameters from the library. All the dimensions are in nanometers. (b) A typical plot of *MSD* values evaluated using the library for the simulated unknown height target with line width of 146.2 nm and line height of 233.8 nm.

### 3.6 TSOM method is Robust to Optical Aberrations and Process Variation

For metrology applications, it is important to evaluate the robustness of the differential TSOM image method. All optical tools have a degree of optical aberration. Knowing the degree to which error is introduced in the measurement by an optical aberration is critical. We studied this using simulations for overlay measurement of an in-chip overlay target [11]. TSOM images were simulated under two conditions: without optical aberration and with third order spherical

aberration (with Zernike coefficient of 0.01). The optical intensity simulated with the programmed spherical aberration was considerably different from the aberration-free profile. However, the evaluated *MSD* corresponding to overlay under the two conditions showed a very small variation of about 0.0004 nm for a 4 nm overlay. The error in the overlay measurement is negligible under the experimental conditions, indicating this method is robust to optical aberration as long as the aberration remains constant between the compared TSOM images.

In practice, process variations that produce small changes in the dimensions of the metrology targets are common, including for overlay measurement targets [11]. For a 4 nm overlay, the selected target in Reference 11 produced an *MSD* value of  $21.7 \times 10^{-6}$ . A 5 nm change in the line height due to process variations produced an *MSD* value of  $22.3 \times 10^{-6}$ , which results in a 0.06 nm error in the overlay measurement. Similarly, simulated 4 nm difference in the linewidth produced an overlay error of 0.032 nm. This example shows a relatively small error in the overlay measurement due to process variations, and hence makes this method robust for the conditions studied in Reference 11.

## 4 TWO TYPES OF APPLICATIONS

Currently, based on the characteristics of the TSOM images, we propose two applications of the TSOM method:

- (i) To determine differences in dimensions, and
- (ii) To determine the absolute dimensions of a target

The first type of application, sensitivity to dimensional change, requires a minimum of two targets. For these sensitivity measurements, although simulations are not necessary, they can greatly enhance the understanding of the dimensional sensitivity behavior pattern of the method.

In the second type of application, an acquired TSOM image is compared with either a simulated or experimentally created library. The best matched TSOM image in the library provides the physical dimensions of the target. Creating a library experimentally requires a set of reference calibration samples (accurately measured with other reference techniques) that span the range of anticipated values for the parameters to be measured by TSOM. Determining the physical dimensions using simulated library, on the other hand, requires accurate simulations, validated by satisfactory experiment-to-simulation agreement during the development phase. In the current work, three types of optical simulation programs were used [4-6], but rigorous experiment to simulation matching has not yet been generally demonstrated.

## 5 SOME EXAMPLE APPLICATIONS

### 5.1 Dimensional Analysis of Nanodots (Nanoparticles, Quantum Dots) Using Experimental Library

We conducted an experiment to determine the size of nanodots using a measured library. For this purpose, approximately square Si nanodots on a Si substrate were fabricated with nominal sizes ranging from 40 nm to 150 nm and a fixed height of about 70 nm. The SEM lateral dimension reference measurements were always larger than the nominal designed dimensions. Even though the nanodots are not exactly the same as nanoparticles, the measurement procedure remains the same. Lateral dimensions of the nanodots were measured using an SEM, which has a nominal measurement uncertainty of about 5 %. Following the SEM measurements, the TSOM images were acquired for the selected nanodots using polarized illumination at a wavelength of 546 nm. A typical background intensity-normalized to zero TSOM image for TE polarization is shown in Fig. 6(a). Using the experimental TSOM images thus created, integrated mean square intensities (MSIs) for the selected nanodots were evaluated and plotted as a function of the SEM-measured nanodot size as shown in Fig. 6(b). Under the current experimental conditions, the curve nominally follows a linear trend. This is treated as the library or the calibration curve for dimensional analysis of nanodots of unknown size. An “unknown-size” nanodot was measured from this calibration curve using the integrated mean square intensity of its TSOM image, producing a measured size of 108 nm. This “unknown-size” nanodot had previously been measured with SEM producing an measured size of 103 nm. Considering this an initial attempt, the agreement is good.

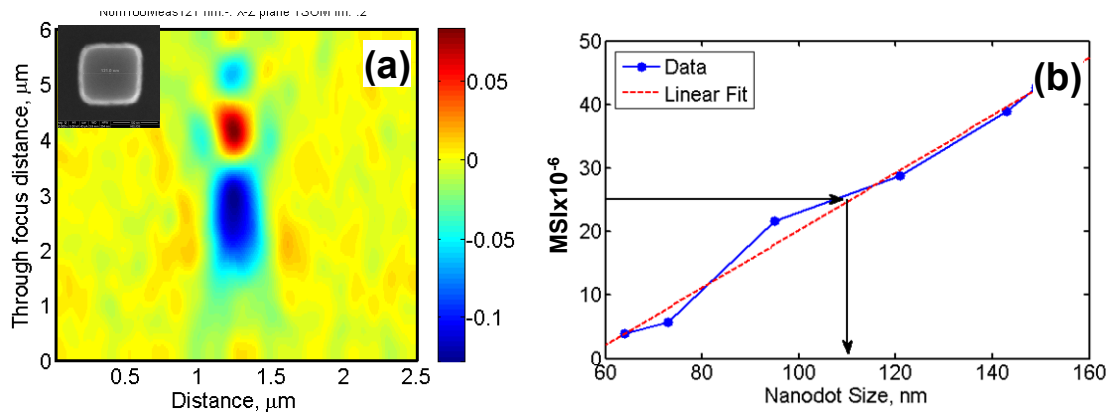


Figure 6. (a) SEM image of a 121 nm nanodot and its experimental intensity-normalized TSOM image (Wavelength = 546 nm, TE Polarization, Illumination NA = 0.27, Collection NA = 0.8, Si nanodot on Si substrate). (b) Experimental mean square intensities of the normalized TSOM images of the selected square nanodots showing a linear trend with size. Arrow marks indicate the experimental size determination of a nanodot of unknown size using the library/calibration curve.

## 5.2 CD Analysis of Dense Line Gratings

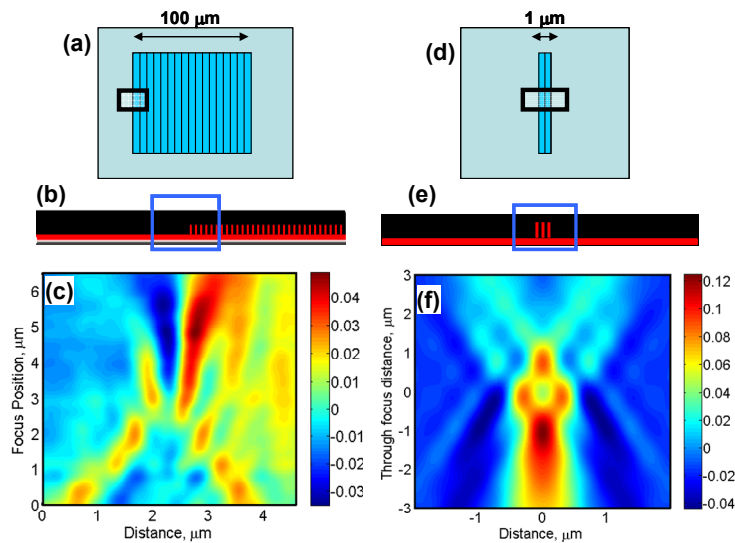


Figure 7. (a) and (b) Location of TSOM analysis for large dense gratings shown in two views. (c) Experimental differential TSOM image at the edge for 3.2 nm difference in the CD using  $\lambda = 546$  nm (AFM measured CDs are 118.5 nm and 115.2 nm, Pitch = 300 nm and Line height = 230 nm, Illumination NA = 0.27, Collection NA = 0.8), (d) and (e) Proposed smaller area line gratings shown in two views, and (f) Simulated differential TSOM image for one nanometer difference in the line width using  $\lambda = 546$  nm (Linewidths = 17 nm and 16 nm, Pitch = 48 nm (1:2) and Line height = 60 nm)

Although dense, uniform line gratings with pitch below one-half the wavelength of the illumination result in an uninteresting featureless TSOM image when the grating fills the field of view, CD analysis with TSOM is still possible if the edge of the grating is analyzed as shown in Fig. 7(a-c). It is recognized that the dimensions of the lines at the edge of a grating are usually different from the lines in the middle of the grating, however, this does demonstrate a way to use the TSOM method to access some potentially-useful dimensional analysis information, even for dense gratings. The experimental differential TSOM image for an AFM-measured 3.2 nm difference in the linewidths shows a good signal (see Fig. 7(c)). Consequently, we proposed a much smaller size line grating as shown in Fig. 7(d) for dimensional analysis. The simulated differential TSOM image for a nanometer difference in the linewidths shows a good signal (Fig. 7(f)), indicating that the smaller sized gratings are equally effective for dimensional analysis using the TSOM method. Advantages include the ability to use much smaller sized gratings, which use less valuable area, and the ability to extend the use of visible wavelength illumination and optics for measuring dense

gratings with linewidths potentially down to as small as 16 nm (with 1:2 pitch), as listed in the *International Technology*

Roadmap for Semiconductors out to 2025. Further experimental verification work is needed to come to a definite conclusion.

### 5.3 Defect Analysis

Under certain circumstances, the use of the direct (not differential) TSOM image is helpful. For example, TSOM images can highlight the presence of defects and the types of defects in a dense grating. Experimental TSOM images for four dense gratings fabricated with intentional defects are shown in Fig 8. The four types of defects with periodic 10 nm differences in the linewidths produce distinctly different TSOM images, indicating the presence of the defects and pointing to the type. In contrast, the absence of any defects would produce featureless TSOM images for these dense targets.

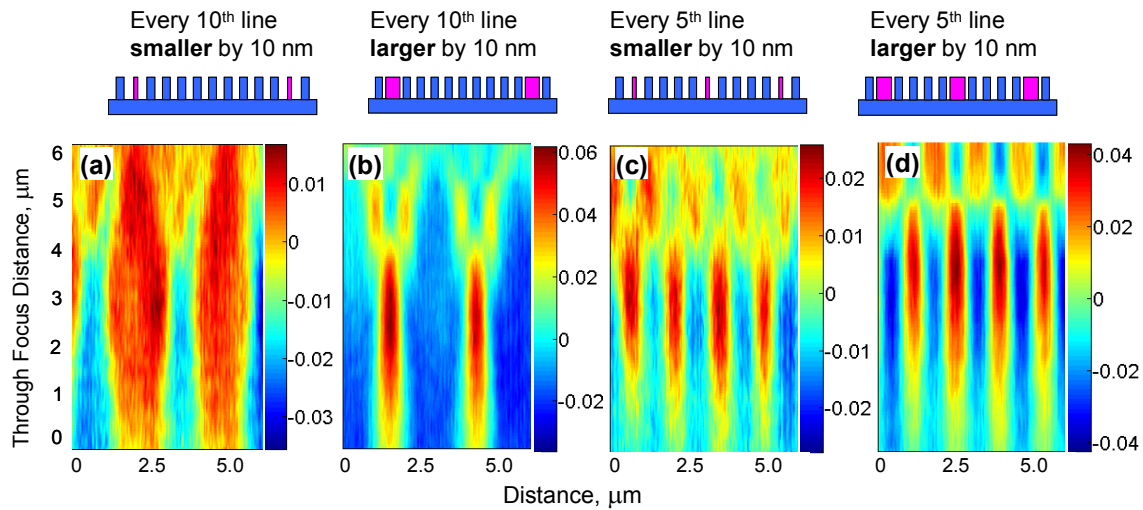


Figure 8. Experimental TSOM images for dense line gratings fabricated with intentional defects.  $\lambda = 546$  nm, nominal line width = 100 nm, nominal pitch = 300 nm, illumination NA = 0.36, imaging NA = 0.8.

## 6 SUMMARY

This paper presents a novel through-focus scanning optical microscopy (TSOM) method that potentially transforms a conventional optical microscope into a 3D metrology tool with nanometer measurement sensitivity, comparable to typical scatterometry, SEM, and AFM. It achieves this by using the additional information contained in a set of through-focus optical images rather than just a single image at the best focus position. The TSOM images are formed by stacking the through-focus optical image intensity profiles such that the  $x$ -axis represents the lateral distance on the target, the  $y$ -axis represents the through-focus position and the intensity of the image, and the  $z$ -axis represents the optical intensity. We have proposed two main applications of the TSOM images: (i) to determine a change in the relative dimensions and (ii) to determine the actual dimensions of a target. We presented several examples using optical simulations and experimental results.

Differential TSOM images appear to be distinct for different parametric changes. They enable us to identify which parameter is different between two targets. However, the differential TSOM images obtained for different magnitude changes of the same parameter appear qualitatively similar. In this case, the  $MSD$  value enables us to determine the magnitude of the difference in the dimension. The TSOM images enable us to determine the dimensions of an unknown target by the library matching method, if we are able to generate accurate simulations and verified by experimental measurement results for a fully characterized optical microscope. We expect the TSOM method to be applicable to a wide variety of targets with a variety of applications including, but not limited to, CD metrology, overlay metrology, defect analysis, inspection, and process control.

## 7 ACKNOWLEDGEMENTS

The NIST Office of Microelectronics Programs, and an Exploratory Project from the Manufacturing Engineering Laboratory, are gratefully acknowledged for financial support. The authors thank SEMATECH and CNST of NIST for target fabrication and measurement support; Richard Silver for permitting us to use NIST's optical microscope and for helpful discussions during through-focus focus metric studies; James Potzick, Benjamin Bunday, Erik Novak, Andrew Rudack, Thomas Germer, Michael Stocker, Bryan Barnes, and Yeung Joon Sohn for their direct or indirect assistance and helpful discussions.

## 8 REFERENCES

- [1] Instrumentation and Metrology for Nanotechnology, Report of the National Nanotechnology Initiative (2004), [http://www.nano.gov/NNI\\_Instrumentation\\_Metrology\\_rpt.pdf](http://www.nano.gov/NNI_Instrumentation_Metrology_rpt.pdf).
- [2] Lojkowski W, Turan R, Proykova A, and Daniszewska A 2006 Nanometrology. Eighth Nanoforum Report  
Nanoforum, [http://www.nano.org.uk/members/MembersReports/NANOMETROLOGY\\_Report.pdf](http://www.nano.org.uk/members/MembersReports/NANOMETROLOGY_Report.pdf).
- [3] Schwenke H, Neuschaefer-Rube U, Pfeifer T, and Kunzmann H, Optical Methods for Dimensional Metrology in Production Engineering: Annals of the CIRP (Elsevier) 51 685-98 (2002).
- [4] Mark Davidson, "Analytic waveguide solutions and the coherence probe microscope," Microelectronic Engineering 13 523-26 (1991).
- [5] T.V. Pistor, 2001 Electromagnetic Simulation and Modeling with Applications in Lithography, Ph.D. Thesis Memorandum No. UCB/ERL M01/19.
- [6] Germer, T., and Marx, E. Proc. SPIE 6152, 61520I1, (2006).
- [7] Attota, R., Silver R.M., and Potzick, J., "Optical illumination and critical dimension analysis using the through-focus focus metric," Proc. SPIE, 6289, p. 6289Q-1-10 (2006).
- [8] Attota, R., Silver, R.M., and Barnes, B.M., "Optical through-focus technique that differentiates small changes in line width, line height, and sidewall angle for CD, overlay, and defect metrology applications," Proc. SPIE 6922, 6922OE-1-13, (2008).
- [9] Brown, E., "Nanoscale Dimensioning Is Fast, Cheap with New NIST Optical Technique," NIST Tech Beat, October 28, [http://www.nist.gov/public\\_affairs/techbeat/tb2008\\_1028.htm#tsom](http://www.nist.gov/public_affairs/techbeat/tb2008_1028.htm#tsom) (2008).
- [10] Attota, R., Germer, T.A., and Silver, R.M., "Through-focus scanning-optical-microscope imaging method for nanoscale dimensional analysis," Optics Letters, Vol. 33, Issue 17, pp. 1990-1992 (2008).
- [11] Attota, R.; Stocker, M., Silver, R.M., Alan Heckert; Hui Zhou; Richard Kasica; Lei Chen; Ronald Dixon; George Orji; Barnes, B.M., Peter Lipscomb, "Through-focus scanning and scatterfield optical methods for advanced overlay target analysis," Proc. SPIE Int. Soc. Opt. Eng. 7272, 727214, (2009).
- [12] Attota, R., Germer, T.A., and Silver, R.M., "Nanoscale measurements with a through-focus scanning optical microscope," Future Fab, 30, pp 83-88, (2009).
- [13] Attota, R., and Silver, R.M., "Nanometrology using a through-focus scanning optical microscopy method," Meas. Sci. Technol. 22, pp 024002, (2011).
- [14] Attota, R., Dixon, R.G., Kramar, J.A., Potzick, J.E., Vladar, A.E., Bunday, B., Novak, E., Rudack, A., "TSOM Method for Semiconductor Metrology," Proc. of SPIE Vol. 7971, 79710T (2011).
- [15] Attota, R., "Nanoscale Measurements with the TSOM Optical Method," an on-line presentation from NIST, (2011), <http://www.nist.gov/pml/div681/grp14/upload/tsom-ravikiran-attota.pdf>.
- [16] Attota, R., Silver, R.M., Germer, T.A., Bishop, M., Larrabee, R., Stocker, M., and Howard, L., "Application of through-focus focus-metric analysis in high resolution optical metrology," Proc. SPIE, 5752, 1441 (2005).
- [17] Silver, R.M., Barnes, B.M., Attota, R., Jun, J., Stocker, M., Marx, E., and Patrick, H.J., "Scatterfield microscopy for extending the limits of image-based optical metrology," Applied Optics, Vol. 46, Issue 20, pp. 4248-4257 (2007).
- [18] Germer, T.A., and Marx, E., "Simulations of optical microscope images", Proc. SPIE 6152, 61520I (2006).
- [19] Silver, R.M., Barnes, B.M., Sohn, Y. Quintanilha, R., Hui Zhou, Chris Deeb, Mark Johnson, Milton Goodwin and Dilip Patel, "The limits and extensibility of optical patterned defect inspection", Proc. SPIE 7638, 76380J (2010).